

The Pattern of CN, O, and Na Inhomogeneities on the Red Giant Branch of Messier 5

Graeme H. Smith

University of California Observatories, Lick Observatory, Department of Astronomy & Astrophysics, UC Santa Cruz, 1156 High St., Santa Cruz, CA 95064, USA

graeme@ucolick.org

Payal N. Modi

The Harker School, 500 Saratoga Ave, San Jose, CA 95129, USA

payalmodi14@gmail.com

Katherine Hamren

Department of Astronomy & Astrophysics, UC Santa Cruz, 1156 High St., Santa Cruz, CA 95064, USA

khamren@ucolick.org

ABSTRACT

Data from the literature are used to explore the relation between $\lambda 3883$ CN band strength and the sodium and oxygen abundances of red giants in the globular cluster Messier 5. Although there is a broad tendency for CN-strong giants in this cluster to have higher sodium abundances and lower oxygen abundances than CN-weak giants of comparable absolute magnitude there are some secondary features in these relations. The oxygen abundance $[O/Fe]$ shows a greater range (0.6-0.7 dex) among the CN-strong giants than the CN-weak giants (≈ 0.3 dex). By contrast $[Na/Fe]$ shows a 0.6-0.7 dex range among the CN-weak giants, but a more limited range of 0.3-0.4 dex among the CN-strong giants. The $\lambda 3883$ CN band anticorrelates in strength with $[O/Fe]$ among the CN-strong giants, but there is little, if any, such trend among the CN-weak giants. In contrast, the CN band strength may show a modest correlation with $[Na/Fe]$ among the CN-weak giants, but there is little evidence for such among the CN-strong giants. Neither oxygen or sodium abundance define a continuous relation with CN band strength. Instead, the CN-strong and CN-weak giants overlap in their sodium and possibly their oxygen abundances. At oxygen abundances of $[O/Fe] = 0.20 \pm 0.05$ it is

possible to have both CN-weak and CN-strong giants, although there may be a discontinuity in $[O/Fe]$ between these two groups of stars that has been smeared out by observational errors. Both CN-weak and CN-strong giants populate the sodium abundance range $0.4 \leq [Na/Fe] \leq 0.6$. Messier 5 may be displaying the results of spatially heterogeneous chemical self-enrichment.

Subject headings: Star Clusters and Associations

1. Introduction

The earliest studies of abundance inhomogeneities in globular clusters (GCs) centered around the behavior of absorption bands of CN and CH in the spectra of red giant branch (RGB) and asymptotic giant branch (AGB) stars. Stars occupying near-identical places in the color-magnitude diagram of a globular cluster can display very different strengths in the CN absorption bands at 3883 Å and 4215 Å and/or the 4300 Å G-band feature that is very sensitive to CH absorption (Zinn 1973a,b; Norris & Zinn 1977; Dickens et al. 1979; Norris & Freeman 1979; Norris 1981; Suntzeff 1980; Smith & Norris 1982; Briley et al. 1992; Briley 1997). Globular clusters of both the halo and disk/bulge populations show such phenomena. Studies during the 1980’s revealed that abundance inhomogeneities within GCs extend to the elements O, Na, and Al (e.g., Cohen 1978; Peterson 1980; Norris et al. 1981; Leep et al. 1986), and during the 1990’s the Lick-Texas group studied the anticorrelations between O and Na in the northern globular clusters M15, M92, M3, M13, M5 and M71 (Snedden et al. 1992, 1994; Kraft et al. 1992, 1993; Shetrone 1996). Whereas early efforts concentrated on CN and CH, the use of 8-10 m class telescopes since the mid-1990’s has seen the emphasis in GC inhomogeneity studies shift to elements ranging in atomic number from O to Al (e.g., Kraft et al. 1997; Sneden et al. 1997, 2004; Ivans et al. 1999; Ramírez & Cohen 2002, 2003; Cohen & Melendez 2005; Johnson et al. 2005; Yong & Grundahl 2008; Carretta et al. 2006; 2007; 2009; 2010; 2011; 2012, 2013; Gratton et al. 2007, 2013).

One particular curiosity is that whereas the CN distribution within many GCs is bimodal (e.g., Norris 1987; Kayser et al. 2008; Smolinski et al. 2011) the elements in the O-Al range tend to show much more uniform spreads in abundance, as can be seen for example in Figure 7 of the large study by Carretta et al. (2009). In general, the CN-strong stars in bimodal-CN GCs have been found to have enhanced Na and Al abundances and depleted O abundances relative to CN-weak stars (some of the earliest studies of this trend include Cottrell & Da Costa 1981; Norris & Smith 1983; Norris & Pilachowski 1985; Lehnert et al. 1991; Brown & Wallerstein 1992; and Drake et al. 1992). However, the detailed relationships between the abundances of C and N, on one hand, and O, Na and Al, on the other, have been less well

studied than the relationships among the O-Al elements.

One of the earliest globular clusters in which CN-enhanced red giants were identified is Messier 5 (Osborn 1971; Hesser et al. 1977) based on DDO photometry. Among RGB stars the cluster exhibits a bimodal $\lambda 3883$ CN distribution (Smith & Norris 1983), but a fairly uniform dispersion in the abundances of O and Na (e.g., Carretta et al. 2009). There are a number of data sets in the literature on CN absorption as well as [O/Fe] and [Na/Fe] abundances among evolved stars in Messier 5. These data are used in the present paper to document the relationship between CN band strengths and O and Na abundances of RGB and AGB stars in the cluster. This work builds on an earlier study of Ivans et al. (2001). A detailed investigation of Na and O abundance trends among red horizontal branch stars in Messier 5 has been published by Gratton et al. (2013).

2. The CN Index data

In red giants of Messier 5 the most prominent CN absorption band in the optical spectrum has a bandhead that is located near 3883 \AA , although the 4215 \AA CN band can also be discerned. Consequently the sources of CN information that are used here comprise measurements of the strength of the $\lambda 3883$ band. One of the earliest studies of CN inhomogeneities in M5 is that of Zinn (1977), who did not make quantitative measurements but rather classified the appearance of the $\lambda 3883$ and $\lambda 4215$ CN bands as either normal or strong based upon visual inspection of spectrograms obtained with the KPNO 2.1 m telescope. His work revealed the presence of $\lambda 3883$ CN inhomogeneities in Messier 5.

Spectroscopic indices that quantify the strength of the $\lambda 3883$ CN band relative to nearby comparison regions of the spectrum have been compiled from the following sources: Smith & Norris (1983, 1993), Briley et al. (1992), Briley & Smith (1993), Smith et al. (1997), and Langer et al. (1985, 1992). In all but the last two of these papers measurements are given of an index denoted $S(3839)$ that was originally introduced by Norris et al. (1981). It is defined in the form $S(3839) = -2.5 \log_{10} F_{\text{CN}}/F_{\text{comp}}$, where F_{CN} is the integrated flux or intensity in the spectrum of a red giant across the wavelength range $3846\text{-}3883 \text{ \AA}$ containing the CN absorption feature, while F_{comp} is the integrated flux or intensity in a comparison region $3883\text{-}3916 \text{ \AA}$ that is reasonably free of CN absorption. Langer et al. (1985) presented two different $\lambda 3883$ CN indices which they designated as m_{CN} and $m_{\text{CN}}(3883)$. Of these it is their m_{CN} measurements that have been used here because this index is defined in a similar manner to $S(3839)$, except that the CN feature and comparison wavelength ranges are $3850\text{-}3878 \text{ \AA}$ and $3896\text{-}3912 \text{ \AA}$ respectively. Langer et al. (1992) measured an index denoted by them as $m(\text{CN})$ that compared the $\lambda 3883$ CN absorption in the wavelength range $3850\text{-}3885$

Å to a combination of flux in the comparison intervals 3650-3780 Å and 4020-4130 Å.

Thus CN indices have been obtained from seven different literature sources. It is necessary to check for zero-point differences in the index systems of these various papers. We have sought to place the indices from other papers onto the system of Smith & Norris (1983; SN83) simply because of their larger sample. The Smith & Norris (1993; SN93) $S(3839)$ indices (from their Table 1) were already transformed onto the SN83 system. Where there are stars in common between SN83 and SN93 the latter $S(3839)$ values are to be preferred since they have MMT or AAT measurements averaged with the SN83 values. Further adopted are the relations $S(3839)[\text{SN83}] = S(3839)[\text{Briley \& Smith 1993}]$ and $S(3839)[\text{SN83}] = 0.1 + S(3839)[\text{Smith et al. 1997}]$ following a discussion in Smith et al. (1997). There are 6 stars in common between the data sets of SN83, Briley et al. (1992; B92), and Langer et al. (1985; LKF85) that have been used to assess the relations between their CN index systems. These are the stars designated by Arp (1955) as I-50, II-50, III-52, III-59, IV-4 and IV-36. Excluding star II-50, for which there is a large difference of 0.16, the mean value of the difference $S(3839)[\text{SN83}] - S(3839)[\text{B92}]$ is -0.0014 , and for the purposes of this paper it is assumed that the $S(3839)$ indices from B92 are on the same system as SN83. Comparing the $S(3839)$ indices of SN83 with the m_{CN} data of LKF85, and again excluding II-50, there is an average difference of $\langle S(3839)[\text{SN83}] - m_{\text{CN}}[\text{LKF85}] \rangle = 0.006$. This offset is used to transform the CN indices of LKF85 onto the system of SN83. Converting the $m(\text{CN})$ indices of Langer et al. (1992; LSK92) is based on one star, Arp II-85, that is common to the study of Briley & Smith (1993; BS93). For this star $S(3839)[\text{BS93}] - m(\text{CN})[\text{LSK92}] = -1.298$. Since the $S(3839)$ indices of BS93 are taken to be on the same scale as SN83, the Langer et al. (1992) values of $m(\text{CN})$ were converted to the SN83 system of $S(3839)$ via this offset of -1.298 . Upon transforming all CN indices onto the $S(3839)$ system of Smith & Norris (1983) equal weight was given to all measurements in forming average values of $S(3839)$, with the exception noted above that where $S(3839)$ data were available from both the SN93 and SN83 papers the former was chosen in place of the latter.

The CN data sources employed here typically identified the stars in their observing programs according to the nomenclature in the color-magnitude diagram study of Arp (1955). Consequently the Arp designations are used in this paper. The V and $B - V$ photometry for stars with Arp (1955) designations was taken from Sandquist & Bolte (2004). In the case of stars S344 and S445 the photometry adopted is that tabulated by Smith & Norris (1993) based on unpublished values from M. Simoda. The reddening and apparent distance modulus was adopted from the 2003 version of the catalog of globular cluster properties described by Harris (1996): $E(B - V) = 0.03$ and $(m - M)_V = 14.46$.

Table 1 contains the data that have been compiled for this paper. Star designations

given in column 1 are those of Arp (1955). Absolute visual magnitudes and dereddened $(B - V)_0$ colors based on the photometry of Sandquist & Bolte (2004) are given in columns 2 and 3, except for stars S344 and S445 as discussed above. Column 4 contains a list of the merged values of the $S(3839)$ $\lambda 3883$ CN index.

There are eleven stars in Table 1 for which the listed value of $S(3839)$ is based on measurements taken from two or three literature sources. Such instances are denoted with a footnote in the table. For small samples of 2 or 3 measurements the ratio of the range R to the standard deviation σ in a measured quantity can be taken as 1.128 and 1.693 respectively (Snedecor 1946; Montgomery 1996). An estimate of the uncertainty representative of the $S(3839)$ data for stars with multiple measurements was calculated from these R/σ ratios and the range in the individual transformed $S(3839)$ values. The mean value thereby derived for $\sigma[S(3839)]$ is 0.03. Uncertainties in the measurements of $S(3839)$ from the published studies of Messier 5 are typically found to be $\sigma \sim 0.02$ - 0.06 mag (Smith & Norris 1983; Briley et al. 1992; Briley & Smith 1983). Various comparisons studied by Langer et al. (1992) indicate that $\sigma[m(\text{CN})] \sim 0.03$ - 0.04 .

Over much of the magnitude range of interest the red giant branch and the asymptotic giant branch are well separated in the color-magnitude diagram (CMD) of M_V versus $(B - V)_0$ shown in Figure 1. There are 46 stars with $S(3839)$ index values in Table 1 of which 10 are AGB stars on the basis of their position in Fig. 1. Stars considered to be in the RGB and AGB phases of evolution are shown as filled squares and open squares respectively. The classification of each star is listed in column 8 of Table 1.

The behavior of the CN index $S(3839)$ versus M_V is shown in Figure 2. At any given magnitude there is considerable scatter in CN index among the RGB stars, which are depicted with filled and open circles according to whether the $\lambda 3883$ CN band is considered to be strong or weak respectively. As first noted in Smith & Norris (1983) the CN distribution on the red giant branch of Messier 5 is bimodal, in fact, this cluster is one of the archetype examples of CN-bimodality among Galactic globular clusters. There is one star in Fig. 2 that is represented by an eight-pointed symbol rather than a circle, this RGB star is IV-34 and may be an example of a red giant with intermediate CN band strength. In addition to the scatter at a given absolute magnitude, both the CN-weak and CN-strong stars exhibit a behavior of increasing mean $S(3839)$ with increasing luminosity on the RGB, which can be attributed at least in part to the sensitivity of the CN band strength to photospheric effective temperature. Based on Fig. 2 a reasonable lower envelope to the RGB-star data is one that passes through the points $(S(3839), M_V) = (0, 0)$ and $(0.2, -2.0)$. Thus a suitable baseline in Fig. 2 above which most RGB stars fall has an equation $S(3839)_b = -0.10M_V$. Residuals $\Delta S(3839) = S(3839) - S(3839)_b$ were calculated relative to this baseline for all

stars listed in Table 1. The $\Delta S(3839)$ index is an attempt to provide a measure of $\lambda 3883$ CN band strength that has been compensated to at least first order for the differences in effective temperature among the RGB stars in the sample. This type of empirical correction has been used often in the literature going back to studies such as Norris et al. (1981). Values of $\Delta S(3839)$ are tabulated in column 5 of Table 1 for both RGB and AGB stars, although it must be stressed that the baseline used to produce these residuals is defined largely by RGB stars.

Asymptotic giant branch stars are plotted in Fig. 2 as either triangles or three-pointed symbols. Two AGB stars (filled triangles) fall among the CN-strong RGB stars in Fig. 2, while one AGB star (open triangle) sits among the CN-weak RGB stars. However, six of the AGB stars have $M_V \sim -1$ and are located at intermediate positions between the CN-weak and CN-strong RGB sequences in Fig. 2. An interpretation that the majority of the AGB stars should be classified as CN-intermediate is not necessarily appropriate, however, since at $M_V \sim -1$ the AGB is considerably bluer by 0.07-0.10 mag in $(B - V)$ than the RGB (Fig. 1). As such, these AGB stars are hotter than RGB stars of similar magnitude, and their higher effective temperatures would serve to diminish the CN band strength relative to that of a RGB star of comparable luminosity. When the AGB and RGB stars are instead compared in a plot of $S(3839)$ versus $(B - V)_0$, as shown in Figure 3 (within which the symbols are the same as in Fig. 2), those AGB stars seemingly of intermediate CN strength on the basis of Fig. 2 now appear to be more consistent with an extrapolation of the CN-strong RGB sequence. Thus, there may also be a bimodal CN distribution among the AGB stars in Messier 5, but the effect is muted in a plot of CN index versus absolute magnitude.

3. The Sodium and Oxygen Abundance Data

Sodium and oxygen abundances were compiled from two sources: Ivans et al. (2001), denoted I01 in the following text, and Table 6 of Carretta et al. (2009), henceforth designated as C09. The former source contains $[\text{Na}/\text{Fe}]$ and $[\text{O}/\text{Fe}]$ measurements that were derived from high-resolution echelle spectra acquired with either the HIRES spectrometer on the Keck I telescope or the Hamilton spectrometer on the Shane 3 m telescope of Lick Observatory. The C09 abundances were downloaded from the electronic database of the VizieR Catalog Server (Table J/A+A/505/117) maintained by the Strasbourg Astronomical Data Center (Ochsenbein et al. 2000). They are based on spectra obtained with the FLAMES/GIRAFFE high-resolution multi-fiber spectrograph on the VLT UT2 telescope (Pasquini et al. 2002). Together these two sources provide a considerable overlap of sodium and oxygen abundance measurements with the CN dataset of Table 1. Oxygen and sodium abundances for M5

giants are also available from Ramírez & Cohen (2003) but CN indices are not available for many of the stars in their study.

A comparison between the [O/Fe] abundances of Carretta et al. (2009) and Ivans et al. (2001) is shown in Figure 4. Measurements by I01 that are based on Keck/HIRES observations are shown as filled circles while those derived from Lick/Hamilton spectra are depicted as open circles. If the entire sample of I01 abundances are considered then a modest offset between the C09 and I01 abundances is derived, such that the mean difference from 12 stars is $\Delta[\text{O/Fe}](\text{C09} - \text{I01}) = 0.07$ with a standard deviation of $\sigma = 0.16$ dex. By contrast, if just the Keck observations of I01 are considered then $\Delta[\text{O/Fe}](\text{C09} - \text{I01}[\text{Keck}]) = 0.12$ and $\sigma = 0.15$ dex for 8 stars, while for the I01 Lick observations alone $\Delta[\text{O/Fe}](\text{C09} - \text{I01}[\text{Lick}]) = -0.04$ and $\sigma = 0.12$ dex for 4 stars. For the purposes of obtaining a combined data set of oxygen abundances it is considered on the basis of these comparisons that the Lick [O/Fe] abundances of I01 are on the same system as that of C09, while the Keck [O/Fe] values of I01 can be placed on the system of C09 by increasing them by 0.12 dex. A homogeneous set of [O/Fe] values was thereby compiled for stars in Table 1 on an abundance scale corresponding to that of Carretta et al. (2009). In the case of stars II-85 and IV-47 the I01 abundances based on their Keck HIRES spectroscopy are adopted as opposed to their reanalysis of Lick 3 m Hamilton echelle spectra.

A consideration of [Na/Fe] reveals evidence for larger offsets between the abundance scales of C09 and I01, as shown in Figure 5. The mean offset between the C09 and I01[Keck] measurements is $\Delta[\text{Na/Fe}](\text{C09} - \text{I01}[\text{Keck}]) = 0.23$ with $\sigma = 0.09$ dex for 8 stars, while for the Lick-based abundances of I01 the offset is $\Delta[\text{Na/Fe}](\text{C09} - \text{I01}[\text{Lick}]) = 0.42$ with $\sigma = 0.22$ dex for 4 stars. Thus the Keck and Lick [Na/Fe] abundances of Ivans et al. (2001) have been transformed onto the abundance scale of Carretta et al. (2009) by adding 0.23 dex and 0.42 dex respectively. The systematic difference between the C09 and I01 sodium abundances partly reflects the application of non-LTE corrections to [Na/Fe] by Carretta et al. (2009), whereas no such corrections were employed by Ivans et al. (2001).

Carretta et al. (2009) reported star-to-star errors in their [O/Fe] and [Na/Fe] determinations of 0.14 dex and 0.08 dex respectively, upon taking into account contributions due to uncertainties in effective temperature T_{eff} , surface gravity, microturbulent velocity v_t , cluster metallicity, and absorption line equivalent width EW . They found that the main contributing sources of error in the oxygen and sodium abundances are errors in T_{eff} , v_t and EW .

Ivans et al. (2001) do not quote formal uncertainties in their [Na/Fe] and [O/Fe] determinations. One can use the numbers given in their Table 3 to estimate the uncertainties that would result from a combination of the typical errors in T_{eff} , surface gravity, v_t , cluster

metallicity, distance modulus, and stellar mass. These factors contribute to uncertainties of 0.08 dex in both [O/Fe] and [Na/Fe]. However, such estimates do not take into account the errors of measurement in O or Na absorption line equivalent widths, and so can only be considered as lower limits to the uncertainties in the [O/Fe] and [Na/Fe] abundances from their study. Ivans et al. (2001) have two stars, II-85 and IV-47, for which they obtained abundances from both Keck/HIRES and Lick/Hamilton spectra. For these two stars they obtain [O/Fe] abundances of +0.08 and +0.02 from Keck and +0.23 and +0.14 from Lick spectra. The [Na/Fe] abundances are +0.38 and +0.17 from Keck and +0.26 and +0.07 from Lick. The data internal to the I01 study are consistent with uncertainties in their [O/Fe] and [Na/Fe] measurements of ~ 0.10 -0.15 dex.

Based on the transformations described in the previous two paragraphs homogenized sets of sodium and oxygen abundances have been compiled for those 40 stars in Table 1 that were studied by either Ivans et al. (2001) and/or Carretta et al. (2009). The homogenized values of [O/Fe] and [Na/Fe] are listed in columns 6 and 7 of Table 1. Of this sample oxygen and/or sodium abundances were measured for 21 stars by Carretta et al. (2009), and their results are listed in columns 9 and 10. Six of the stars in Table 1 having either [O/Fe] or [Na/Fe] determinations are considered to be AGB members of Messier 5.

4. The Relation Between CN Band Strength and Oxygen Abundance

The $\Delta S(3839)$ CN residual is plotted in Fig. 6 versus the merged [O/Fe] abundance data from column 6 of Table 1, with filled and open symbols denoting RGB and AGB stars respectively. There is a clear difference in the mean oxygen abundances of the CN-strong and CN-weak giants, with the former having the lower average [O/Fe], in accord with the previous finding of Ivans et al. (2001). Among the CN-strong population of RGB stars ($\Delta S(3839) \geq 0.30$) there is an anticorrelation between CN band strength and [O/Fe]. Thus the CN-strong giants are themselves not a homogeneous population but have a dispersion in both $\Delta S(3839)$ and [O/Fe], with the oxygen abundance extending over a range of at least 0.6 dex. The CN-weak RGB stars ($\Delta S(3839) \leq 0.20$) exhibit a smaller range in [O/Fe] of ≈ 0.35 dex, and there is no clear CN-O anticorrelation within Fig. 6 among the CN-weak population. What is striking from Fig. 6 is that near the transition in oxygen abundance between CN-strong and CN-weak stars, which occurs at [O/Fe] $\approx +0.2$ dex, there are a number of red giants that have nearly the same [O/Fe] yet very different $\lambda 3883$ CN band strengths. It is almost as if the CN-strong and CN-weak RGB stars define offset sequences in Fig. 6, which are displaced in $\Delta S(3839)$ by about 0.3 mag at [O/Fe] = 0.2, and which overlap over a narrow range in [O/Fe]. The one CN-intermediate RGB star identified in

Fig. 2, Arp IV-34 with $\Delta S(3839) = 0.21$, has an oxygen abundance of $[O/Fe] = +0.13$, and falls near the offset region in Fig. 6.

Six AGB stars are represented in Fig. 6. One of them is an oxygen-rich CN-weak star, while three others fall close to the sequence defined by the CN-strong RGB stars. Two AGB stars (I-55 and III-53) stand out as having low oxygen content and relatively weak CN bands for their M_V magnitude. They appear to fall on an extrapolation of the CN-weak RGB sequence to depleted oxygen abundances. However, as noted in Sec. 2, the relatively weak CN bands may be a consequence of the higher effective temperature of these AGB stars relative to their RGB counterparts of comparable absolute magnitude. Thus the outlying positions of I-55 and III-53 in Fig. 6 may be a temperature effect.

In Figure 7 the CN residual $\Delta S(3839)$ is again plotted against oxygen abundance except that this plot shows only the $[O/Fe]$ abundances from Carretta et al. (2009) that are listed in column 9 of Table 1. In this figure there will be no scatter in $[O/Fe]$ due to uncertainties in the I01-to-C09 transformations. Nonetheless, the offset between CN-strong and CN-weak RGB stars near $[O/Fe] = 0.2$ is still conspicuous in Fig. 7, and the range in $[O/Fe]$ abundance among the CN-weak giants is still on the order of 0.30-0.35 dex. There may be a modest overlap in oxygen abundance between the CN-weak and CN-strong groups evident in Figs. 6 and 7, however this overlap of ~ 0.1 dex is comparable to the observational uncertainties in the $[O/Fe]$ determinations. As such, the data cannot rule out the possibility that there is a discontinuity in $[O/Fe]$ between the CN-strong and CN-weak giants that has been smeared out in Figs. 6 and 7 by observational errors.

Whereas in broad terms it can be concluded that the CN-strong RGB stars in Messier 5 have lower $[O/Fe]$ abundances than the CN-weak red giants, the situation is modified by the fact that (i) there is a spread of more than 0.6 dex among the CN-strong giants, and (ii) there is a population of red giants that have $[O/Fe] \sim +0.2$ but nonetheless very different $\lambda 3883$ CN band strengths.

The empirical anticorrelation between CN band strength and oxygen abundance seen in Figs. 6 and 7 suggests that relative to the atmospheres of the CN-weak giants the material in the CN-strong stars has been subject to the O \rightarrow N cycle of hydrogen burning. If the CN-strong stars contain within their atmospheres material that was initially like that of the CN-weak giants, but which has been subjected to the O \rightarrow N process of hydrogen burning, then a factor of 10 or more enhancement in nitrogen abundance might be found among the CN-strong giants.

The CN-weak giants in Messier 5 are worthy of additional study. It would be valuable to identify a larger sample of such stars and to document the range in $[O/Fe]$ among them,

so as to determine whether there is an anticorrelation between CN band strength and $[O/Fe]$ within this population. The nitrogen abundances of the CN-strong giants may have been enhanced in part by a contribution from the C→N cycle of hydrogen burning in addition to the action of the O→N process within some initial CNO abundance mix. There is modest evidence of a CN-CH anticorrelation on the RGB of Messier 5 (Smith & Norris 1983), however, their data are in part based on photographic spectra, and a modern CCD study of carbon abundances among both CN-weak and CN-strong giants aimed at determining the precise relations between C, N, and O abundances would be another worthwhile pursuit. Cohen et al. (2002) did uncover a CN-CH anticorrelation among stars on the lower half of the red giant branch of Messier 5. A spectrum synthesis analysis is needed to determine whether the total C+N+O abundance is the same or different in the CN-strong and CN-weak giants.

5. The Relation Between CN Band Strength and Sodium Abundance

Figures 8 and 9 contain plots of the $\Delta S(3839)$ CN residual versus $[Na/Fe]$ abundances from columns 7 and 10 respectively of Table 1. Thus the sodium abundances in the larger sample of Fig. 8 are from the merging of the I01 and C09 data sets, whereas only the C09 abundances are used in Fig. 9. Filled and open squares again denote RGB and AGB stars respectively. It is clear from both figures that the CN-strong stars as a population have higher mean sodium abundances than the CN-weak stars, again consistent with the earlier findings of Ivans et al. (2001). Most CN-strong giants observed in Messier 5 have sodium abundances of $[Na/Fe] \geq +0.4$, whereas many of the CN-weak giants have $[Na/Fe]$ less than 0.4. However, there are some additional interesting features.

The CN-strong giants exhibit a 0.4 dex range in $[Na/Fe]$, and the majority of them have $[Na/Fe] \leq 0.7$. By contrast the CN-weak giants exhibit a notably wider spread in $[Na/Fe]$ of ≈ 0.7 dex. There may be a mild trend in Fig. 8 for the $\Delta S(3839)$ residual to correlate with $[Na/Fe]$ among the CN-weak red giants, which is perhaps better seen in Fig. 9 despite the smaller number of stars. Among the CN-strong RGB stars there is a smaller range in $[Na/Fe]$ and no evidence of a CN-Na correlation. The sodium abundance range of $0.4 \leq [Na/Fe] < 0.6$ is populated by both CN-strong and CN-weak giants, and it is possible to identify pairs of CN-strong and CN-weak giants that have identical sodium abundances within the observational uncertainties. It appears that the CN-strong and CN-weak sequences in Fig. 8 overlap by 0.2 dex in $[Na/Fe]$, but that they are offset by ~ 0.2 mag in the $\Delta S(3839)$ residual. This conclusion might in part be a consequence of uncertainties in the L01-C09 transformations smearing out the $[Na/Fe]$ values around 0.4 dex in Fig. 8.

Nonetheless, in Fig. 9 where only the $[\text{Na}/\text{Fe}]$ abundances from Carretta et al. (2009) are used, two CN-weak RGB stars with $[\text{Na}/\text{Fe}] > 0.35$ overlap the CN-strong giants in sodium abundance.

6. Discussion

The behavior of oxygen and sodium as a function of the CN band strength of red giants in Messier 5 shows some interesting contrasts. Whereas $[\text{O}/\text{Fe}]$ shows a greater range among the CN-strong giants than the CN-weak giants, $[\text{Na}/\text{Fe}]$ shows a greater range among the CN-weak giants. The CN band strength anticorrelates with $[\text{O}/\text{Fe}]$ among the CN-strong giants, but there is little tendency of such among the CN-weak giants. By contrast, although the CN band strength may show some modest correlation with $[\text{Na}/\text{Fe}]$ among the CN-weak giants, there is little evidence for a CN-Na correlation among the CN-strong giants. What is common in the case of both oxygen and sodium is that there is not a continuous relation between CN band strength and either $[\text{O}/\text{Fe}]$ or $[\text{Na}/\text{Fe}]$. Rather the CN-strong and CN-weak giants overlap in their range of both sodium and possibly oxygen abundance (sodium more so than oxygen).

On the basis of the $[\text{Na}/\text{Fe}]$ versus $[\text{O}/\text{Fe}]$ diagram, Carretta et al. (2009) divided the stars in Messier 5 into three groups. Primordial stars (or “first-generation” or P stars in their terminology) were defined as those with $[\text{Na}/\text{Fe}] \leq 0.1$; such stars also tend to have $[\text{O}/\text{Fe}] > 0.2$. Among the enriched stars (or “second-generation” stars in the terminology of C09) Carretta et al. (2009) drew a dividing line between an intermediate (I) and an extreme (E) component that has the equation $[\text{Na}/\text{Fe}] = [\text{O}/\text{Fe}] + 0.9$. The most extreme of the enriched stars have $[\text{Na}/\text{O}] > 0.9$ along with $[\text{Na}/\text{Fe}] > 0.5$, and these represent only a small fraction of the stars in Messier 5. The bulk of the enriched stars have $[\text{O}/\text{Fe}] > -0.3$ and $0.6 > [\text{Na}/\text{Fe}] > 0.1$. According to Figs. 8 and 9 the “first-generation” P stars of Carretta et al. (2009) are all CN-weak. There are 5 stars in Table 1 which on the basis of the $[\text{Na}/\text{Fe}]$ abundances listed in column 7 would be classified in the P group of Carretta et al. (2009). The mean and standard deviation in $\Delta S(3839)$ for these stars are 0.04 and 0.03 respectively, which is typical of the giants with the weakest $\lambda 3883$ CN bands in Messier 5. Of the 27 stars in Table 1 that fall into the intermediate I group the mean and standard deviation in $\Delta S(3839)$ are 0.26 and 0.18 respectively; whereas for the extreme E group with $[\text{Na}/\text{O}] > 0.9$ (on the basis of columns 6 and 7 of Table 1) the mean $\Delta S(3839)$ is 0.44 with a standard deviation of 0.12. Thus, the P, I, and E groups of Carretta et al. (2009) have progressively larger mean CN residuals.

What is interesting, however, is that the CN-weak population of giants with $\Delta S(3839) <$

0.2 does include quite a number of stars that would be classified in the “second-generation” I group by Carretta et al. (2009) on the basis of having sodium abundances of $[\text{Na}/\text{Fe}] > 0.1$, e.g., stars such as I-68, II-39, III-36 and IV-19. If we consider CN-weak giants to be those with $\Delta S(3839) \leq 0.2$ then the $[\text{Na}/\text{Fe}]$ abundance varies from -0.1 to 0.6 dex among these stars. Thus the sodium abundances of the CN-weak giants extend well into the range in $[\text{Na}/\text{Fe}]$ typical of C09’s group I. There are no C09 group E stars among the CN-weak giants. Among the CN-strong giants with $\Delta S(3839) \geq 0.3$ the lowest value of $[\text{Na}/\text{Fe}]$ is 0.10 for star II-50, which falls right at the boundary of C09’s groups P and I. These comparisons emphasize the point made in Section 5 concerning the overlap of sodium abundances between CN-strong and CN-weak giants.

The pattern of abundances in Messier 5 might be interpreted within a context whereby CN-strong giants formed from gas of different initial composition to that of the CN-weak stars. Cohen et al. (2002) showed that star-to-star CN band variations extend to the base of the RGB at $M_V \sim +3$ in Messier 5, consistent with the variations being of a very early or primordial origin.¹ One suggestion on the basis of the CN-O anticorrelation of Fig. 6 is that the CN-strong stars might have formed from gas that was initially identical to that of the CN-weak giants, but was processed through the CNO bicycle of hydrogen burning before becoming incorporated into the CN-strong stars themselves. Dating back to a suggestion by Cottrell & Da Costa (1981) it has become common to view the interiors of intermediate-mass AGB stars (e.g., Fenner et al. 2004; Ventura & D’Antona 2008a, 2008b, 2009; Decressin et al. 2009), or even more massive stars (e.g., Smith 2006; Decressin et al. 2007), formed at early times within a globular cluster, as the sites for such additional CNO-processing prior to CN-strong star formation.

Whereas the abundances of C, N, and O are the product of the CNO bicycle reactions of hydrogen burning, the element sodium can be manufactured in a Ne-Na proton-addition cycle that takes place at temperatures at which the CNO bicycle also occurs (e.g., Langer et al. 1993; Cavallo et al. 1996). The action of the Ne-Na cycle in bringing about a significant build up of sodium appears to have occurred within the confines of the CN, O, Na composition range prevalent among the CN-weak giants. In other words, some stars in Messier 5 formed with an initial enrichment in Na that was not accompanied by a great

¹On top of the complexities of primordial enrichment there is the added complication of interior mixing within the red giants of Messier 5. The dredge-up of CNO-processed material can alter the original composition of both CN-strong and CN-weak giants. Whereas such additional processing could increase the nitrogen surface abundances of both CN-weak and CN-strong giants, which would act to strengthen the CN bands, it would also reduce the surface carbon abundance, thereby having an opposing effect of diminishing the CN band strengths.

enough enhancement in nitrogen as to cause them to exhibit strong CN bands on the red giant branch. Other stars may have formed with comparable sodium abundances but high enough nitrogen as to become CN-strong red giants. Similarly, two stars might have formed in Messier 5 with similar oxygen abundances of $[O/Fe] \sim 0.15-0.25$ yet one with much lower nitrogen abundance than the other, such as to lead to a CN-weak and CN-strong pair once the stars evolved onto the red giant branch.

Messier 5 seems to be a cluster in which there is not a unique one-to-one relationship between N abundance on one hand (as traced by CN band strength on the RGB) and O and Na abundances on the other hand. Perhaps what Messier 5 is indicating is that the self-enrichment of this cluster was the by-product of spatially heterogeneous enrichment by intermediate-mass or high-mass stars having a range of ages and formation times.

This research has made use of the VizieR and SIMBAD catalog access tools, CDS, Strasbourg, France. We thank the referee for useful comments on the manuscript. G. H. S. gratefully acknowledges support from the National Science Foundation through grant AST-0908757.

REFERENCES

- Arp, H. C. 1955, *AJ*, 60, 317
- Briley, M. M. 1997, *AJ*, 114, 1051
- Briley, M. M., & Smith, G. H. 1993, *PASP*, 105, 1260 (BS93)
- Briley, M. M., Smith, G. H., Bell, R. A., Oke, J. B., & Hesser, J. E. 1992, *ApJ*, 387, 612 (B92)
- Brown, J. A., & Wallerstein, G. 1992, *AJ*, 104, 1818
- Carretta, E., Bragaglia, A., Gratton, R. G., Leone, F., Recio-Blanco, A., & Lucatello, S. 2006, *A&A*, 450, 523
- Carretta, E., Bragaglia, A., Gratton, R. G., Lucatello, S., & D’Orazi, V. 2012, *ApJ*, 750, L14
- Carretta, E., Bragaglia, A., Gratton, R. G., Lucatello, S., & Momany, Y. 2007, *A&A*, 464, 927
- Carretta, E., Gratton, R. G., Bragaglia, A., D’Orazi, V., & Lucatello, S. 2013, *A&A*, 550, 34
- Carretta, E., Lucatello, S., Gratton, R. G., Bragaglia, A., & D’Orazi, V. 2011, *A&A*, 533, 69
- Carretta, E., et al. 2009, *A&A*, 505, 117 (C09)
- Carretta, E., et al. 2010, *A&A*, 520, 95
- Cavallo, R. M., Sweigart, A. V., & Bell, R. A. 1996, *ApJ*, 464, L79
- Cohen, J. G. 1978, *ApJ*, 223, 487
- Cohen, J. G., Briley, M. M., & Stetson, P. B. 2002, *AJ*, 123, 2525
- Cohen, J. G., & Meléndez, J. 2005, *AJ*, 129, 303
- Cottrell, P. L., & Da Costa, G. S. 1981, *ApJ*, 245, L79
- Decressin, T., Charbonnel, C., Siess, L., Palacios, A., Meynet, G., & Georgy, C. 2009, *A&A*, 505, 727
- Decressin, T., Meynet, G., Charbonnel, C., Prantzos, N., & Ekström, S. 2007, *A&A*, 464, 1029
- Dickens, R. J., Bell, R. A., & Gustafsson, B. 1979, *ApJ*, 232, 428
- Drake, J. J., Smith, V. V., & Suntzeff, N. B. 1992, *ApJ*, 395, L95

- Fenner, Y., Campbell, S., Karakas, A. I., Lattanzio, J., C., & Gibson, B. K. 2004, MNRAS, 353, 789
- Gratton, R. G., et al. 2007, A&A, 464, 953
- Gratton, R. G., et al. 2013, A&A, 549, 41
- Harris, W. E. 1996, AJ, 112, 1487
- Hesser, J. E., Hartwick, F. D. A., & McClure, R. D. 1977, ApJS, 33, 471
- Ivans, I. I., Kraft, R. P., Sneden, C., Smith, G. H., Rich, R. M., & Shetrone, M. 2001, AJ, 122, 1438 (I01)
- Ivans, I. I., Sneden, C., Kraft, R. P., Suntzeff, N. B., Smith, V. V., Langer, G. E., & Fulbright, J. P. 1999, AJ, 118, 1273
- Johnson, C. I., Kraft, R. P., Pilachowski, C. A., Sneden, C., Ivans, I. I., & Benman, G. 2005, PASP, 117, 1308
- Kayser, A., Hilker, M., Grebel, E. K., & Willemsen, P. G. 2008, A&A, 486, 437
- Kraft, R. P., Sneden, C., Langer, G. E., & Prosser, C. F. 1992, AJ, 104, 645
- Kraft, R. P., Sneden, C., Langer, G. E., & Shetrone, M. D. 1993, AJ, 106, 1490
- Kraft, R. P., Sneden, C., Smith, G. H., Shetrone, M. D., & Langer, G. E. 1997, AJ, 113, 279
- Langer, G. E., Hoffman, R., & Sneden, C. 1993, PASP, 105, 301
- Langer, G. E., Kraft, R. P., & Friel, E. D. 1985, PASP, 97, 373 (LKF85)
- Langer, G. E., Suntzeff, N. B., & Kraft, R. P. 1992, PASP, 104, 523 (LSK92)
- Leep, E. M., Wallerstein, G., & Oke, J. B. 1986, AJ, 91, 1117
- Lehnert, M. D., Bell, R. A., & Cohen, J. G. 1991, ApJ, 367, 514
- Montgomery, D. C. 1996, Introduction to Statistical Quality Control, Wiley
- Norris, J. 1981, ApJ, 248, 177
- Norris, J. 1987, ApJ, 313, L65
- Norris, J., Cottrell, P. L., Freeman, K. C., & Da Costa, G. S. 1981, ApJ, 244, 205
- Norris, J., & Freeman, K. C. 1979, ApJ, 230, L179
- Norris, J., & Pilachowski, C. A. 1985, ApJ, 299, 295
- Norris, J., & Smith, G. H. 1983, ApJ, 272, 635
- Norris, J., & Zinn, R. 1977, ApJ, 215, 74
- Ochsenbein F., Bauer P., & Marcout, J. 2000, A&AS, 143, 23

- Osborn, W. 1971, *Obs*, 91, 223
- Pasquini, L., et al. 2002, *The Messenger*, 110, 1
- Peterson, R. C. 1980, *ApJ*, 237, L87
- Ramírez, S. V., & Cohen, J. G. 2002, *AJ*, 123, 3277
- Ramírez, S. V., & Cohen, J. G. 2003, *AJ*, 125, 224
- Sandquist, E. L., & Bolte, M. 2004, *ApJ*, 611, 323
- Shetrone, M. D. 1996, *AJ*, 112, 1517
- Smith, G. H. 2006, *PASP*, 118, 1225
- Smith, G. H., & Norris, J. 1982, *ApJ*, 254, 149
- Smith, G. H., & Norris, J. 1983, *ApJ*, 264, 215 (SN83)
- Smith, G. H., & Norris, J. E. 1993, *AJ*, 105, 173 (SN93)
- Smith, G. H., Shetrone, M. D., Briley, M. M., Churchill, C. W., & Bell, R. A. 1997, *PASP*, 109, 236
- Smolinski, J. P., Martell, S. L., Beers, T. C., & Lee, Y. S. 2011, *AJ*, 142, 126
- Snedecor, G. W. 1946, *Statistical Methods*, Iowa State College Press
- Snedden, C., Kraft, R. P., Guhathakurta, P., Peterson, R. C., & Fulbright, J. P. 2004, *AJ*, 127, 2162
- Snedden, C., Kraft, R. P., Langer, G. E., Prosser, C. F., & Shetrone, M. D. 1994, *AJ*, 107, 1773
- Snedden, C., Kraft, R. P., Prosser, C. F., & Langer, G. E. 1992, *AJ*, 104, 2121
- Snedden, C., Kraft, R. P., Shetrone, M. D., Smith, G. H., Langer, G. E., & Prosser, C. F. 1997, *AJ*, 114, 1964
- Suntzeff, N. B. 1980, *AJ*, 85, 408
- Ventura, P., & D’Antona, F. 2008a, *A&A*, 479, 805
- Ventura, P., & D’Antona, F. 2008b, *MNRAS*, 385, 2034
- Ventura, P., & D’Antona, F. 2009, *A&A*, 499, 835
- Yong, D., & Grundahl, F. 2008, *ApJ*, 672, L29
- Zinn, R. 1973a, *ApJ*, 182, 183
- Zinn, R. 1973b, *A&A*, 25, 409

Zinn, R. 1977, ApJ, 218, 96

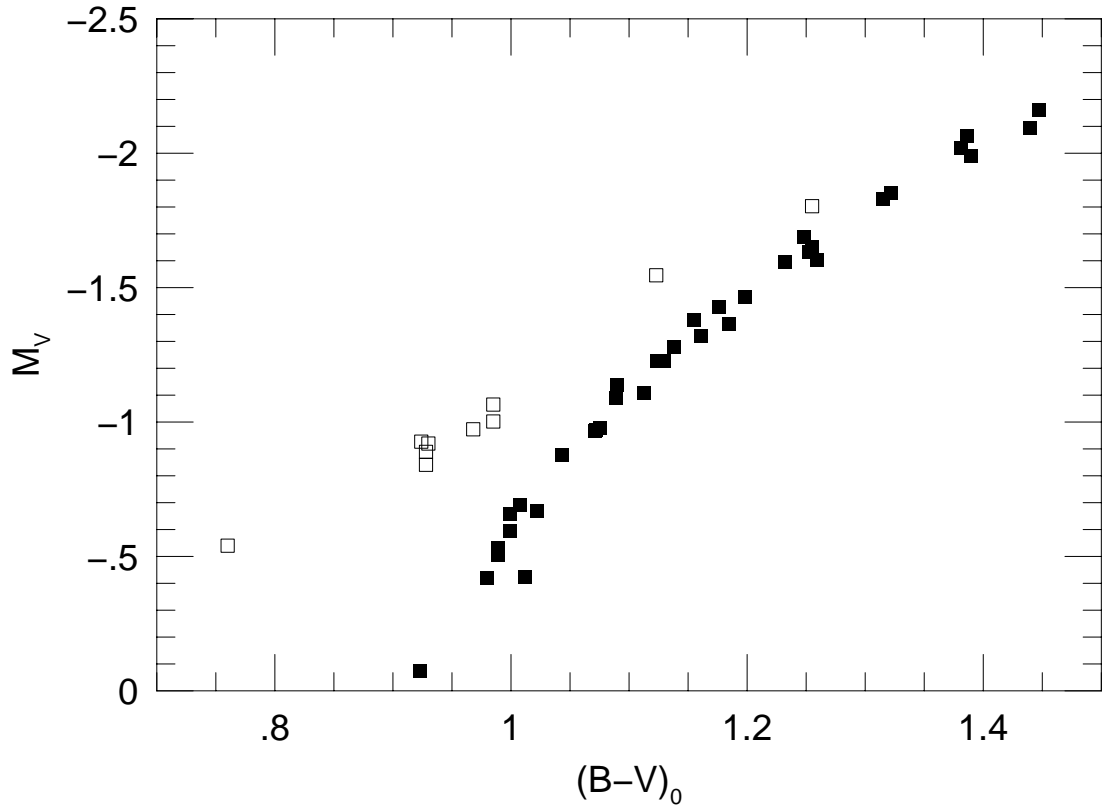


Fig. 1.— The M_V versus $(B - V)_0$ color-magnitude diagram of stars from Messier 5 that are listed in Table 1. Filled symbols correspond to stars considered to be on the red giant branch whereas open symbols denote asymptotic giant branch stars.

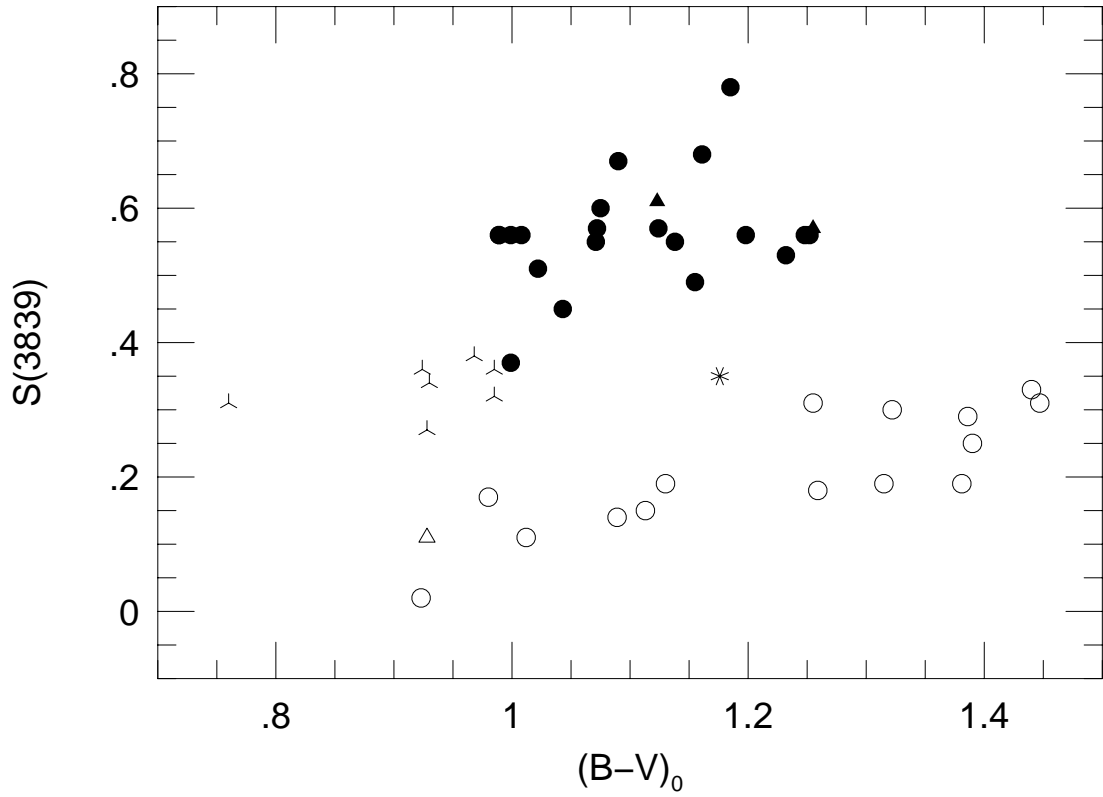


Fig. 3.— The CN index $S(3839)$ versus $(B - V)_0$ for giants in Messier 5. Filled circles, open circles, and the eight-pointed symbol correspond to CN-strong, CN-weak and CN-intermediate RGB stars respectively. Triangles and three-pointed symbols denote AGB stars.

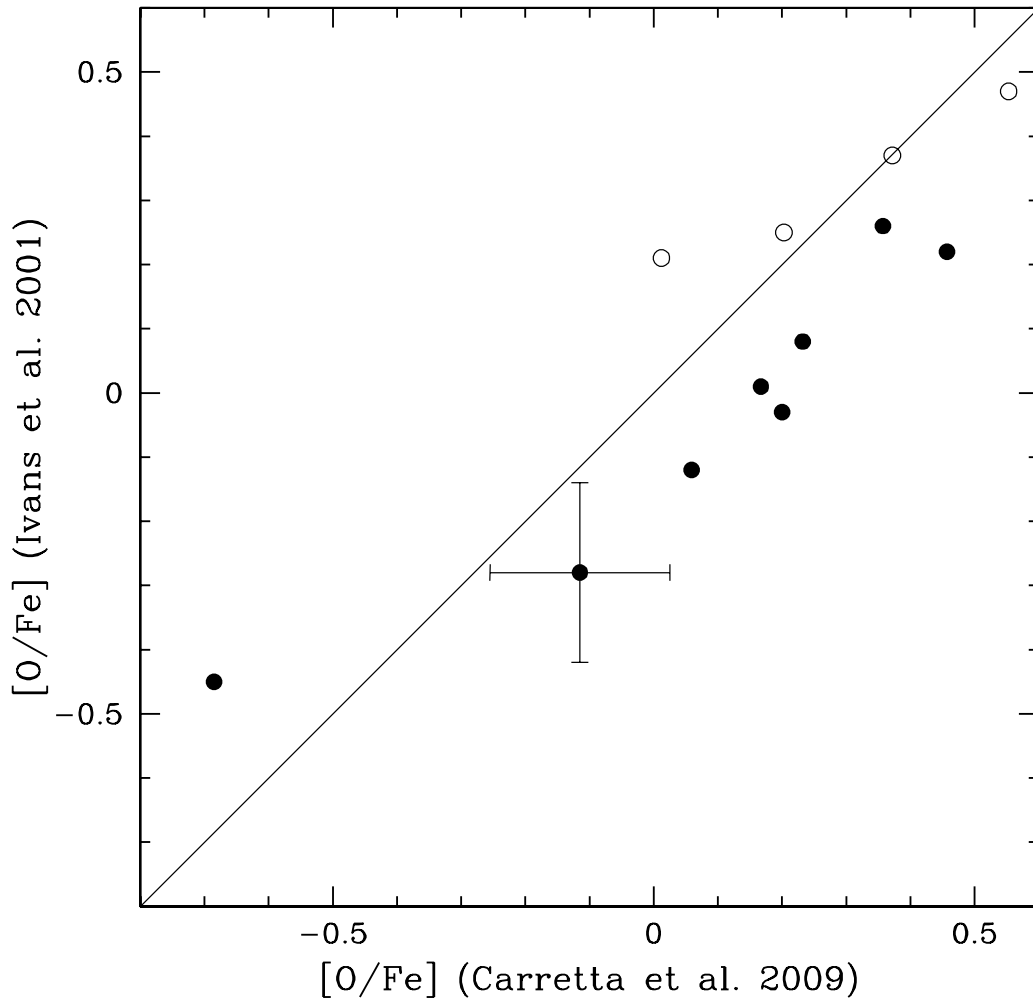


Fig. 4.— Oxygen abundances from Ivans et al. (2001) versus those from Carretta et al. (2009) for stars in common between the two programs. Results from I01 based on HIRES and Hamilton spectrometer data are shown as filled and open symbols respectively. Error bars of length ± 0.14 dex in both the C09 and I01 [O/Fe] abundances are shown for one star.

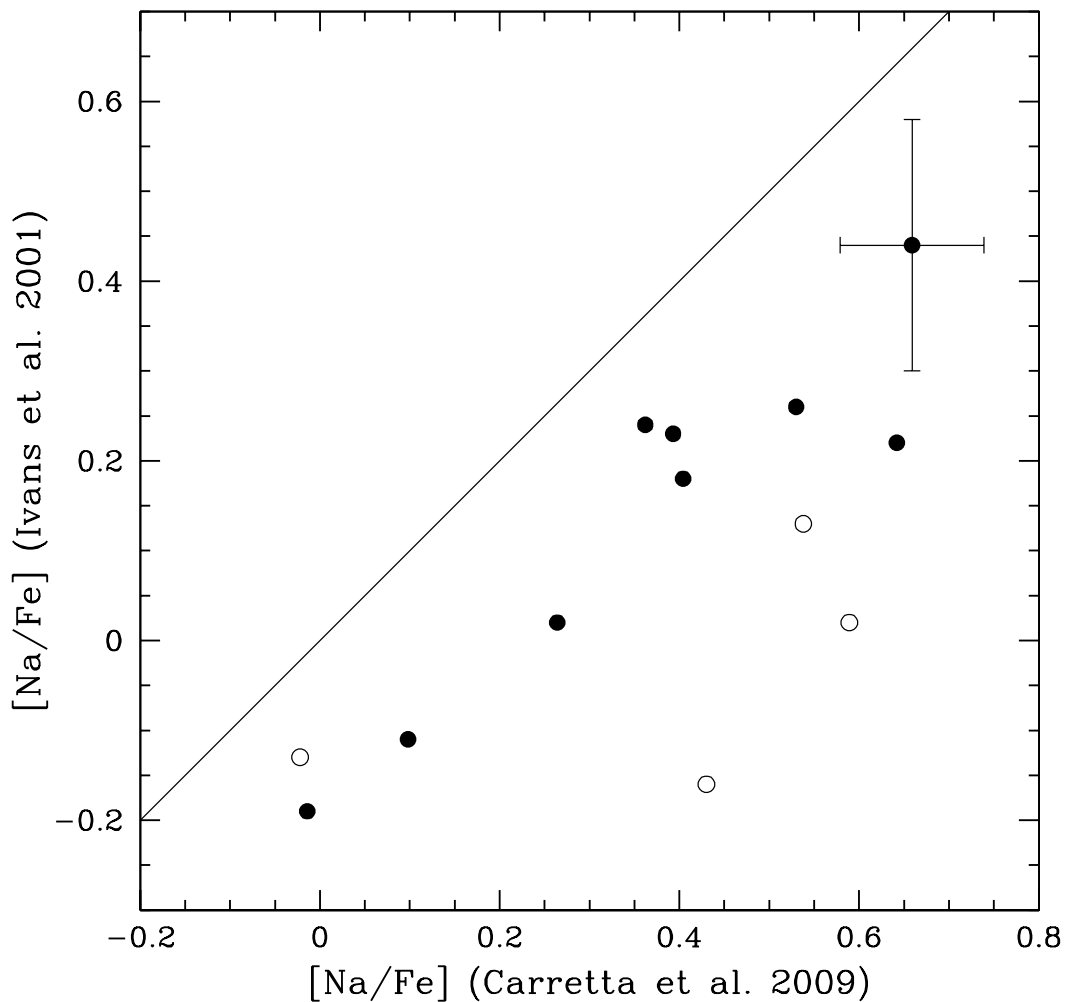


Fig. 5.— Sodium abundances from Ivans et al. (2001) versus those from Carretta et al. (2009) for stars in common between the two programs. Results from I01 based on HIRES and Hamilton spectrometer data are shown as filled and open symbols respectively. Error bars of length ± 0.08 dex and ± 0.14 dex in the C09 and I01 $[\text{Na}/\text{Fe}]$ abundances respectively are shown for one star.

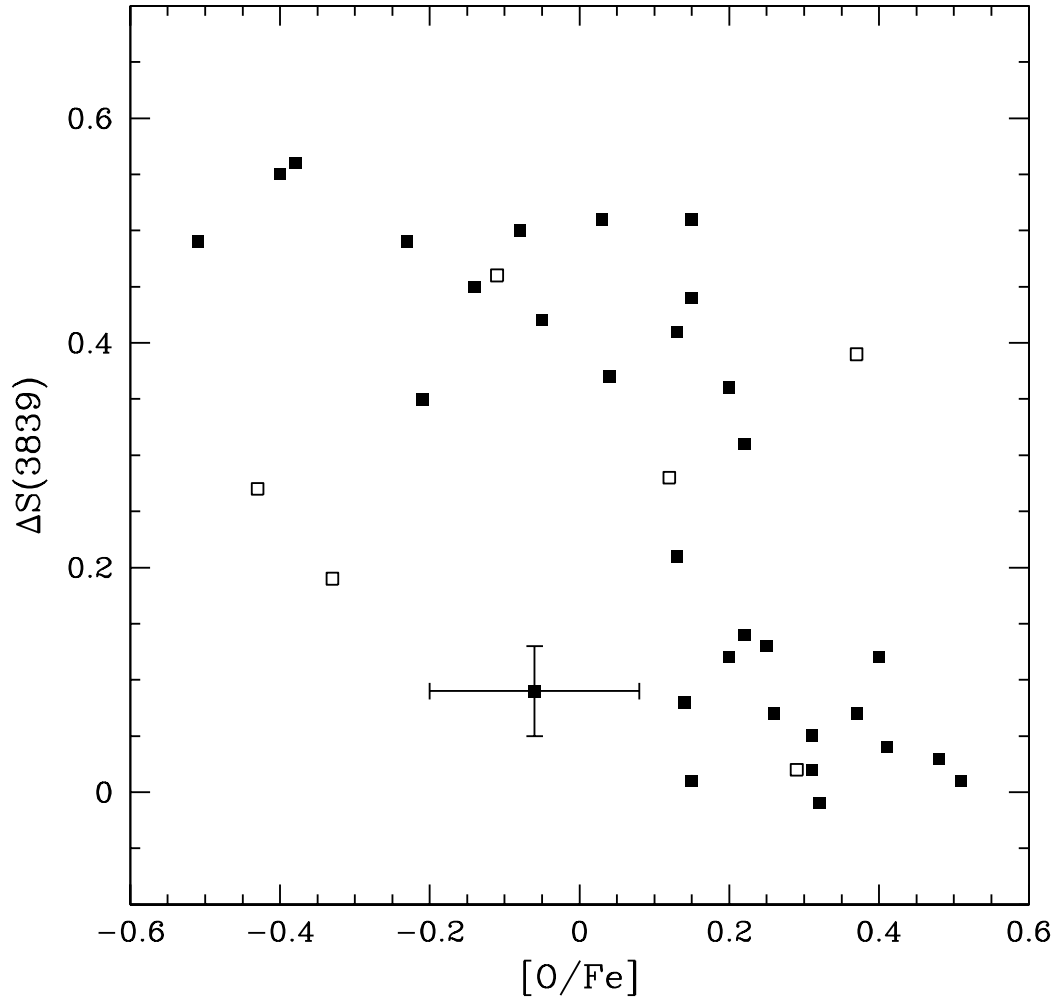


Fig. 6.— The $\lambda 3883$ CN residual $\Delta S(3839)$ versus oxygen abundance from column 6 of Table 1. Filled and open squares denote RGB and AGB stars respectively (as in Fig. 1). A pair of representative error bars of length ± 0.04 in $\Delta S(3839)$ and ± 0.14 dex in $[O/Fe]$ is depicted.

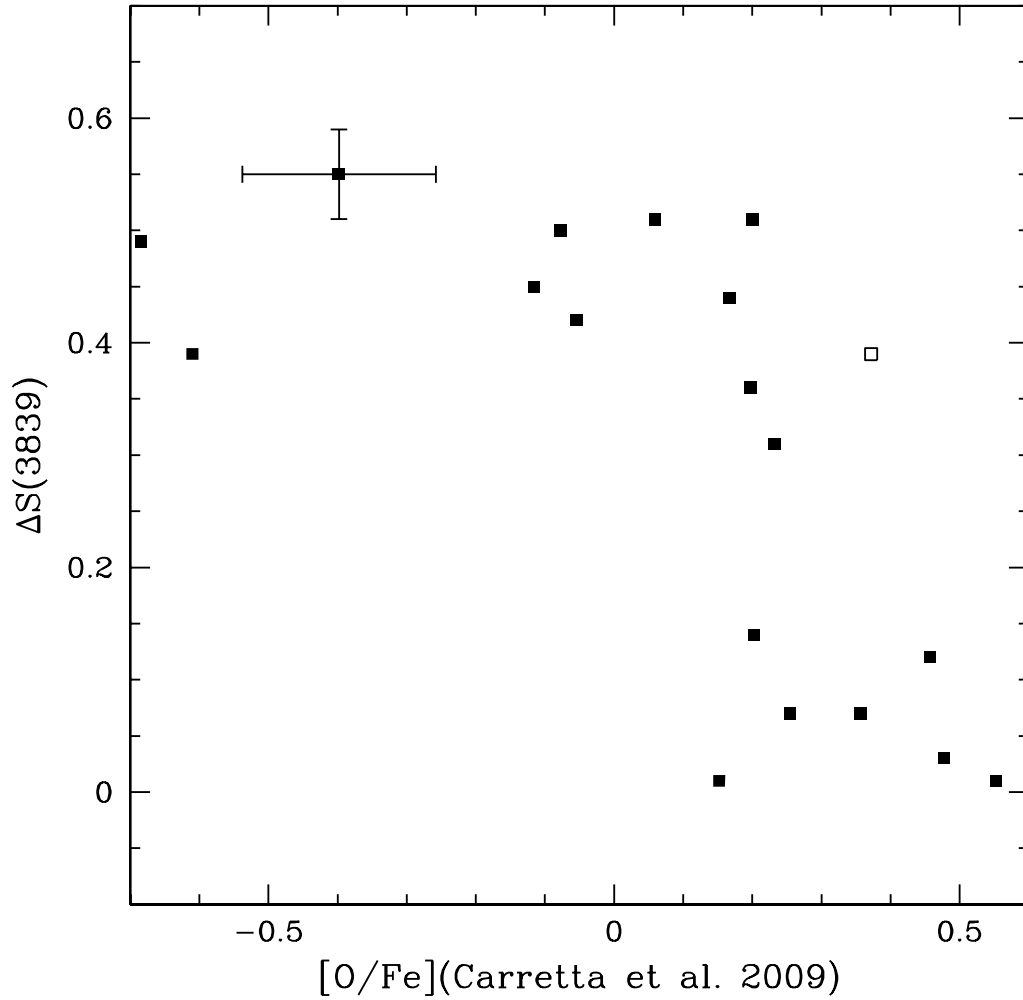


Fig. 7.— The $\lambda 3883$ CN residual $\Delta S(3839)$ versus oxygen abundance from Carretta et al. (2009) as listed in column 9 of Table 1. Filled and open squares denote RGB and AGB stars respectively (see Fig. 1). Error bars of length ± 0.04 in $\Delta S(3839)$ and ± 0.14 dex in the Carretta et al. (2009) oxygen abundance are shown for one star.

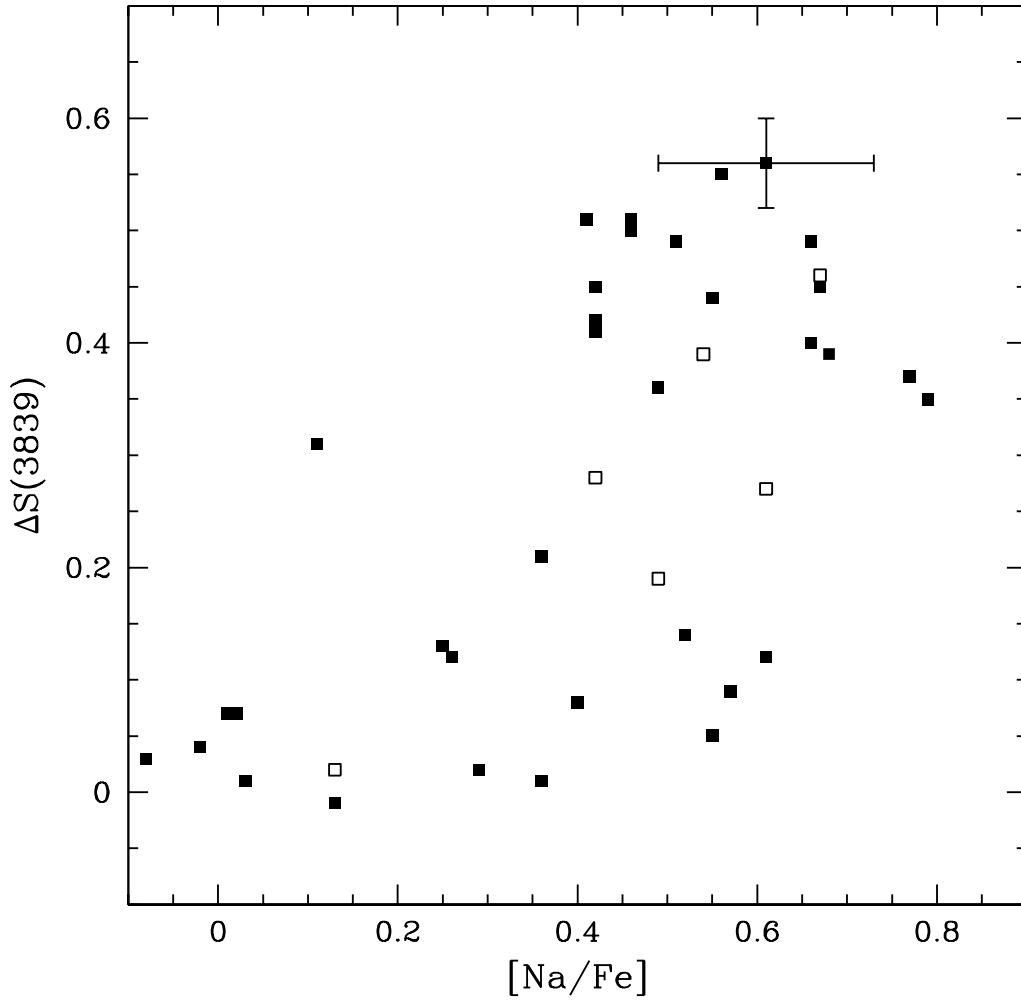


Fig. 8.— The CN residual $\Delta S(3839)$ versus $[Na/Fe]$ from column 7 of Table 1. Filled and open squares denote RGB and AGB stars respectively. A pair of representative error bars of length ± 0.04 in $\Delta S(3839)$ and ± 0.12 dex in $[Na/Fe]$ is included.

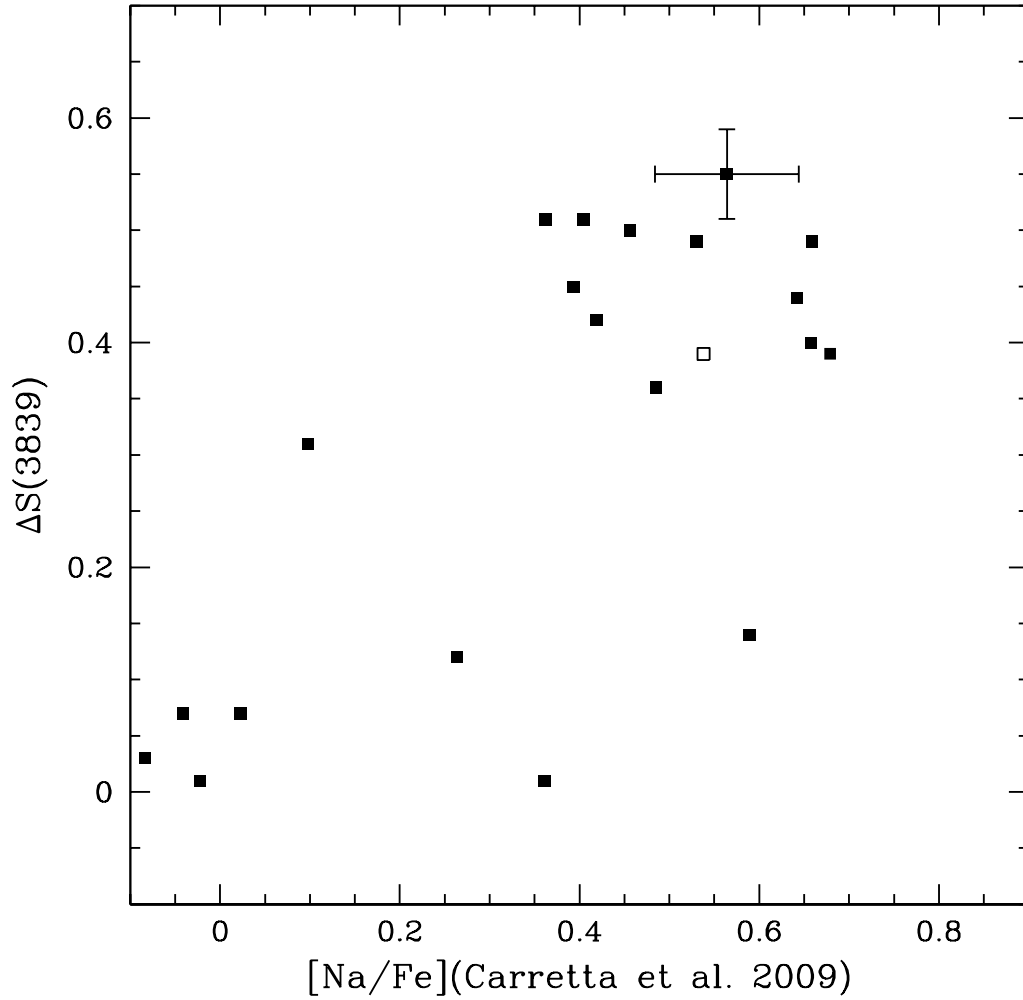


Fig. 9.— The $\Delta S(3839)$ residual versus $[Na/Fe]$ from Carretta et al. (2009) as listed in column 10 of Table 1. Filled and open squares denote RGB and AGB stars respectively. Typical error bars of length ± 0.04 in $\Delta S(3839)$ and ± 0.08 dex in the Carretta et al. (2009) sodium abundance are shown for one star.

Table 1. Data for Evolved Giant Stars in Messier 5

Star (1)	M_V (2)	$(B - V)_0$ (3)	$S(3839)$ (4)	$\Delta S(3839)$ (5)	$[O/Fe]^a$ (6)	$[Na/Fe]^a$ (7)	Class (8)	$[O/Fe](C09)^b$ (9)	$[Na/Fe](C09)^b$ (10)
I-2	-0.67	1.02	0.51	0.44	0.15	0.55	RGB	0.167	0.642
I-4	-1.09	1.09	0.14	0.03	0.48	-0.08	RGB	0.477	-0.084
I-14	-1.46	1.20	0.56	0.41	0.13	0.42	RGB
I-25	-0.88	1.04	0.45	0.36	0.20	0.49	RGB	0.197	0.485
I-39	-1.36	1.19	0.78	0.64	RGB
I-50	-0.66	1.00	0.56 ^c	0.49	-0.51	0.66	RGB	-0.685	0.659
I-55	-0.84	0.90	0.27	0.19	-0.33	0.49	AGB
I-58	-1.23	1.12	0.57	0.45	-0.14	0.42	RGB	-0.115	0.393
I-61	-1.11	1.11	0.15	0.04	0.41	-0.02	RGB
I-68	-1.99	1.39	0.25	0.05	0.31	0.55	RGB
I-71	-1.38	1.16	0.49 ^c	0.35	-0.21	0.79	RGB
II-39	-0.07	0.92	0.02	0.01	0.15	0.36	RGB	0.152	0.361
II-50	-0.59	1.00	0.37 ^c	0.31	0.22	0.11	RGB	0.232	0.098
II-59	-1.14	1.09	0.67	0.56	-0.38	0.61	RGB
II-61	-1.00	0.99	0.36	0.26	AGB
II-74	-0.69	1.01	0.56	0.49	-0.23	0.51	RGB	0.530
II-85	-2.10	1.44	0.33	0.12	0.20	0.61	RGB
II-86	-1.07	0.99	0.32	0.21	AGB
III-3	-2.02	1.38	0.19	-0.01	0.32	0.13	RGB
III-36	-1.65	1.26	0.31	0.14	0.22	0.52	RGB	0.203	0.589
III-50	-1.55	1.12	0.61	0.46	-0.11	0.67	AGB
III-52	-0.42	1.01	0.11 ^c	0.07	0.37	0.01	RGB	0.357	-0.041
III-53	-0.93	0.92	0.36	0.27	-0.43	0.61	AGB
III-59	-0.53	0.99	0.56 ^c	0.51	0.03	0.41	RGB	0.059	0.362
III-67	-0.97	1.07	0.57	0.47	RGB
III-78	-1.83	1.32	0.19 ^c	0.01	0.51	0.03	RGB	0.553	-0.022
III-94	-1.63	1.25	0.56	0.40	0.66	RGB	0.658
III-96	-1.60	1.23	0.53 ^c	0.37	0.04	0.77	RGB
III-99	-1.69	1.25	0.56	0.39	-0.61	0.68	RGB	-0.610	0.679
III-122	-2.16	1.45	0.31	0.09	-0.06	0.57	RGB
IV-4	-0.42	0.98	0.17 ^c	0.13	0.25	0.25	RGB
IV-12	-0.98	1.08	0.60	0.50	-0.08	0.46	RGB	-0.078	0.456
IV-19	-1.85	1.32	0.30	0.12	0.40	0.26	RGB	0.457	0.264
IV-26	-0.90	0.93	0.11	0.02	0.29	0.13	AGB
IV-30	-0.97	0.97	0.38	0.28	0.12	0.42	AGB
IV-34	-1.43	1.18	0.35	0.21	0.13	0.36	RGB
IV-36	-0.51	0.99	0.56 ^c	0.51	0.15	0.46	RGB	0.200	0.404
IV-47	-2.06	1.39	0.29	0.08	0.14	0.40	RGB
IV-49	-1.32	1.16	0.68	0.55	-0.40	0.56	RGB	-0.398	0.564
IV-56	-1.28	1.14	0.55	0.42	-0.05	0.42	RGB	-0.054	0.419
IV-59	-1.80	1.26	0.57 ^c	0.39	0.37	0.54	AGB	0.372	0.538
IV-72	-1.60	1.26	0.18 ^c	0.02	0.31	0.29	RGB
IV-74	-0.97	1.07	0.55	0.45	0.67	RGB
IV-82	-1.23	1.13	0.19	0.07	0.26	0.02	RGB	0.255	0.023
S344	-0.54	0.76	0.31	0.26	AGB

Table 1—Continued

Star (1)	M_V (2)	$(B - V)_0$ (3)	$S(3839)$ (4)	$\Delta S(3839)$ (5)	$[O/Fe]^a$ (6)	$[Na/Fe]^a$ (7)	Class (8)	$[O/Fe](C09)^b$ (9)	$[Na/Fe](C09)^b$ (10)
S445	-0.92	0.93	0.34	0.25	AGB

^aMerged values from the data of Ivans et al. (2001) and Carretta et al. (2009).

^bValues from Carretta et al. (2009).

^cBased on two or three values from the literature.